AWESW2022
21st Australasian Wind Engineering Society Workshop
2 – 3 February, 2023

Velocity fields behind non-uniform passive grid screens in a boundary layer wind tunnel

Yuhui Zhang[1*], and Matthew S. Mason[1]

[1*]*The School of Civil Engineering, The University of Queensland. Email: yuhui.zhang3@uqconnect.edu.au.*

[1]*The School of Civil Engineering, The University of Queensland. Email: matthew.mason@uq.edu.au.*

ABSTRACT

The application of passive grid screens is explored as a cost-effective method to generate thunderstorm downburst-like sheared velocity profile in a boundary layer wind tunnel. An existing approach for designing passive grid screens has been applied and tested for three non-uniform rectangular grid screens. This study investigates flow field characteristics behind these screens and compares results to those behind a square grid screen and the theoretical estimate of the mean velocity field. Experiments were carried out in the University of Queensland wind tunnel. Tests show that as greater shear (i.e. dU/dz) is prescribed in the target mean velocity profile the larger the error between observed and predicted profiles become. For all screens, the observed mean velocity shear in the interior of the tunnel was greater than predicted. The presence of an amplification in velocity near the wall, noted in previous research for square grid screens, was found to be less prominent as the screens became more non-uniform. Turbulence intensity and integral length scale showed less direct dependence on the characteristics of the screen than mean velocities.

1. Introduction

1.1 Background

Existing methods to generate the characteristic “nose” shaped velocity profiles produced during thunderstorm downburst outflows in traditional boundary layer wind tunnels have generally relied upon active-control approaches. For example, this has been done by installing moving or rotating plates or louvres (e.g., Lin & Savory 2006; Butler et al. 2009) or by utilizing muti-fan systems (Butler et al. 2009; Mason et al. 2020). However, there are disadvantages to these active approaches, for example, (1) calibration is often complex and time-consuming, and (2) the physical equipment required is expensive and difficult to incorporate into existing wind tunnels without permanent modifications. As such, it is advantageous to explore the use of passive screens as a cost-effective method that could be adopted by existing boundary layer wind tunnel facilities so they could simulate downburst-like wind fields without major modification.

Zhang and Mason (2022) describe the application of a theoretical model developed by Choi et al. (2016) to design passive gird screens to generate both uniform velocity profiles and downburst-like “nose” shape velocity profiles in a regular wind tunnel. Near-wall amplification of the mean velocity and boundary layer growth along the wind tunnel, which was outside the expectation of Choi’s model, were identified and investigated. Additional systematic deviation from from the desired mean velocity profile was also noted in the measured velocity profiles behind the non-uniform ‘downburst’ screens. Although Choi et al. (2016) successfully validated their design model through a series of wind tunnel and CFD simulations, they did so using screens with narrow slits, and only in the region away from the

wall. Such screen designs are not appropriate for wind engineering applications because the turbulence length scales generated are too small. Because of this and given the prevalence of square grids as standard turbulence-generating features in many wind tunnels (e.g., Vita et al. 2018), the rectangular grid screens used by Zhang and Mason (2022) are seen as more suitable for generating realistic downburst-like velocity fields. This paper extends the work of Zhang and Mason (2022) and seeks to characterise the velocity field behind a series of non-uniform rectangular grid screens designed to generate shear flows. Differences between measured mean velocity fields and those predicted by the Choi et al. (2016) model are highlighted and discussed. Turbulence characteristics are also reported and discussed.

1.2 Choi's theoretical model

Coupling general concepts of the Bernoulli equation and resistance pressure drop, Choi et al. (2016) formulated an efficient baffle design equation that conceptually enables the manipulation of an input velocity field to a desired target velocity field:

$$\left[\frac{1}{\beta(y)^2}-1\right]g(y)^2=\left[\frac{1}{\beta_0^2}-1\right]+[f(y)^2-g(y)^2]C_d^2 \tag{1}$$

where, $f(y)$ is the velocity profile upstream of the screen normalised by the mean velocity over the depth of the wind tunnel; g(y) is the normalized target velocity profile downstream of the screen; $\beta(y)$ is the non-uniform local porosity of the perforated screen; β_0 is the average porosity of the screen; C_d is the discharge coefficient, and y is the vertical distance from the nearest wind tunnel wall. Rearranging this equation, one arrives at Eq (2), which can be used to determine the local screen porosity, $\beta(y)$ needed to produce a desired velocity profile or at Eq (3) to predict the velocity profile behind a screen with known characteristics.

$$\beta(y)=\left\{\frac{\left(\frac{1}{\beta_0^2}-1\right)+\left[f(y)^2-g(y)^2\right]\times C_d^2+g(y)}{g(y)}\right\}^{-\frac{1}{2}} \tag{2}$$

$$g(y)=\left\{\frac{\left(\frac{1}{\beta_0^2}-1\right)+f(y)^2\times C_d^2}{\left(\frac{1}{\beta(y)^2}-1\right)+C_d^2}\right\}^{\frac{1}{2}} \tag{3}$$

2. Experimental Setup and Procedures

All experiments were conducted in the open-circuit wind tunnel in the School of Civil Engineering at The University of Queensland (UQWT). The length (L), width (W) and height (Y) of the wind tunnel test section are 2100 mm × 762 mm × 762 mm, respectively. All the internal surfaces of the wind tunnel are notionally smooth. Screens can be inserted at the inlet of the test section to modify the downstream velocity field. For this study, three non-uniform porosity rectangular grid screens were designed using Eq (3) and mean velocities, turbulence intensity and integral length scales were measured at two different downwind locations along the wind tunnel test section, L1 and L2, which

correspond to x/Y = 1.8 and 2.3, respectively, where x is the distance from the test section inlet to the measurement location. Velocity measurements were also taken behind a uniform screen at the same locations. The grid dimensions (H: hole height; B: bar thickness, excluding the top and bottom bar), distribution, bulk porosity β_0 and screen nomenclature are provided in Table 1. The theoretical target profiles, g(y), behind each of the screens, as determined using Eq (3), are shown in Figure 1.

Table 1. Screen parameters.

Screen	Target profile	Grid Distribution	H [mm]	B [mm]	H/B	β_0
Grid 1	Uniform	9x9	65	19.5	3.33	0.567
Screen 1	SF1	9×9	59 - 66	19.1 - 26	2.27 – 3.45	0.567
Screen 2	SF2	9×9	53 - 71	14.8 - 31	1.71 – 4.8	0.567
Screen 3	SF3	9×9	46 - 76	10.4 - 36	1.28 – 7.3	0.567

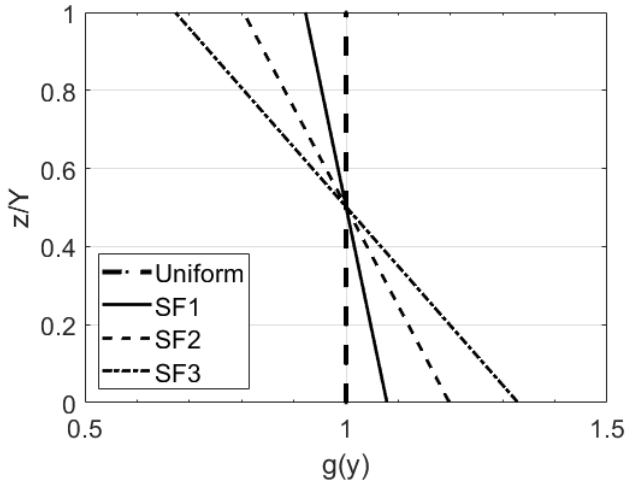

Figure 1. Target normalised velocity profiles.

All velocity measurements were made using a TFI Cobra Probe traversed through the depth of the wind tunnel. Data were sampled for 60 seconds at each test elevation at a sampling frequency of 625 Hz. The wind tunnel inlet velocity was set as 16 m/s. All three velocity components were measured, but only the along-wind component, *U*, is reported in this paper.

3. Results

3.1 Mean velocity field

Figure 2 (a) to (d) show the normalised mean *U* velocity profiles over the height of the test section at L1 and L2 behind Grid 1, Screen 1, Screen 2, and Screen 3. All the profiles are normalised by U_{mean}, which is the mean velocity measured over the height of the test section.

In Figure 2 (a), the measured velocity flow field doesn't show any obvious deviation from the uniform flow target in the middle two-thirds of the wind tunnel. However, flow amplification, as well as boundary layer development, can be observed near the top and bottom walls. In Figure 2 (b), the measured velocity profiles show generally good agreement with the target SF1 profile at both L1 and L2, except again for velocity amplification near the wall and boundary layer development along the tunnel. A small deviation can be observed between the measured profiles and the target in the height range of z/Y = 0.6 – 0.8. This deviation is illustrated as the actual flow generated more shear than the target, which results in a steeper slope on the measured velocity profiles. Figure 2 (c) shows target SF2 profile is less suitably attained than SF1. With the flow shear on the target profile increasing, the

deviation from the target increases. An even larger deviation can be observed in Figure 2 (d) when the highest shear flow, SF3, was set as the target. As Figure 2 (a), (b), (c) and (d) show for all screens, the velocity amplification magnitude decreases while the boundary layer depth of this amplification increases as flow moves downstream from L1 to L2. However, only small differences are observed between L1 and L2 profiles over the height range of z/Y = 0.2 – 0.8, which means the bulk of the profile remains relatively constant throughout the tunnel.

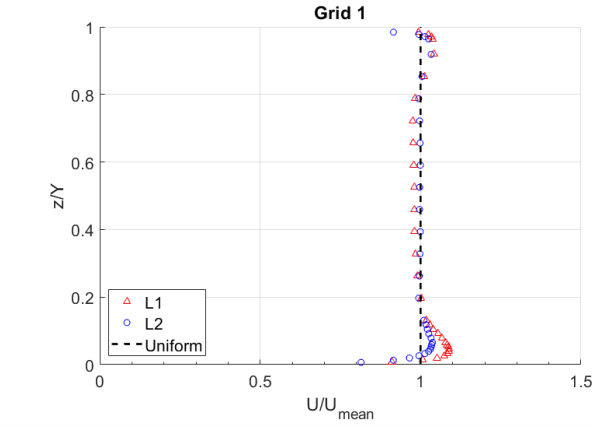

(a) Grid 1 at L1, x/Y = 1.8 and L2, x/Y = 2.3

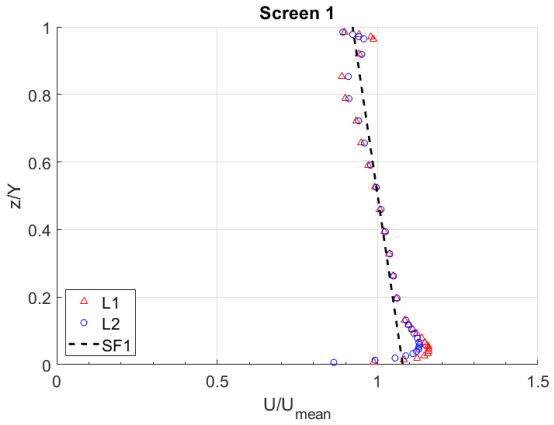

(b) Screen 1 L1, x/Y = 1.8 and L2, x/Y = 2.3

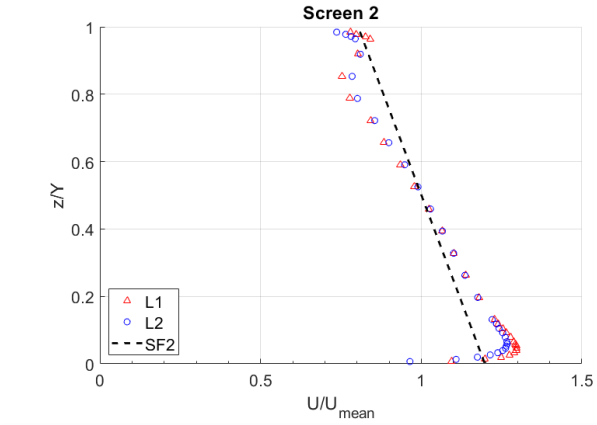

(c) Screen 2 L1, x/Y = 1.8 and L2, x/Y = 2.3

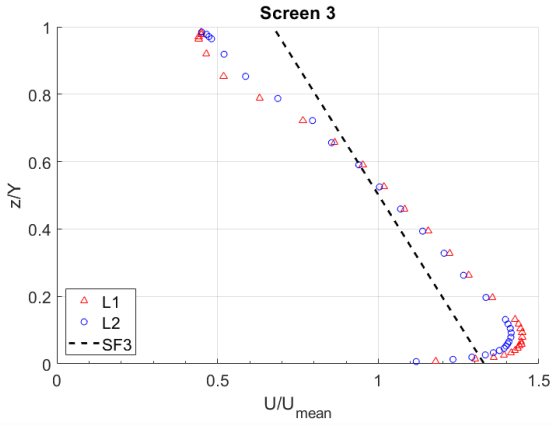

(d) Screen 3 L1, x/Y = 1.8 and L2, x/Y = 2.3

Figure 2. Mean velocity profiles at L1 and L2 behind Grid 1, Screen 1, Screen 2, and Screen 3.

Overall, it is observed that larger velocity shear leads to a larger deviation between the measured velocity field and the theoretical target profile. This deviation tends to higher levels of shear in the interior of the tunnel and reduced presence of the overshoot observed for Screen 3. Given this observation, a correction to Choi's theoretical model is required for use with non-uniform rectangular grids. Future work will explore developing such a correction.

3.2 Turbulence characteristic

Given the importance of turbulent flow characteristics to wind loading, it is also useful to quantify the turbulence characteristic behind each of the screens. Here, the along-wind turbulence intensity, I_u, and length scale, L_u, are reported.

Figure 3 (a) and (b) show the turbulence intensity profile behind Grid 1, Screen 1, Screen 2, and Screen 3. For Screen 1 and 2, the turbulence intensities are around 5 % and are only slightly larger in the region away from the wall. However, for Screen 3, the turbulence intensity shows a sharp increase near the

top of the tunnel where the hole-to-bar thickness ratio decreases under H/B < 2.5. Slightly larger turbulence values are seen in the lower half of the tunnel for the non-uniform screens when compared with Grid 1, but little difference is noted between Screen 1-3. A small reduction in turbulence intensity between L1 and L2 is noted for all screens reflecting a small decay along the tunnel.

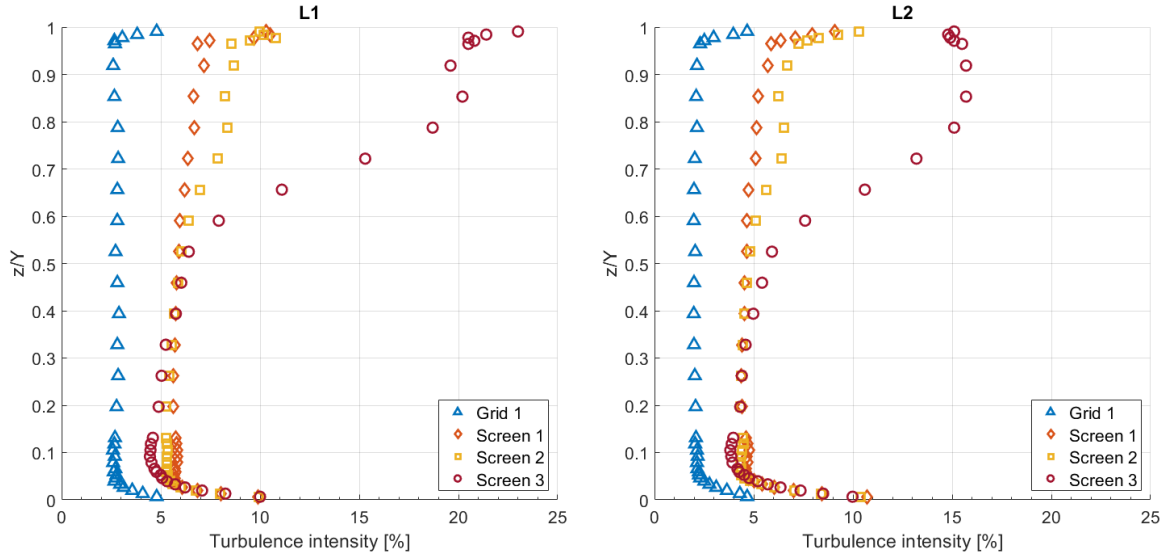

(a) L1, x/Y = 1.8 (b) L2, x/Y = 2.3

Figure 3. Turbulence intensity at L1 and L2 behind Grid 1, Screen 1, Screen 2, and Screen 3.

Figure 4 (a) and (b) show the turbulence length scale distribution over the height of the test section at L1 and L2 behind Screen 1, Screen 2, and Screen 3. Similar to the turbulence intensity, the length scale seems to have a weak relationship to H/B. The length scale is relatively uniform behind both Screen 2 and Screen 3. For Screen 3, the turbulence length scale increases sharply with the decrease of H/B. Referring to Vita et al. (2018), two parameters, hole size and bar thickness on the screen, influence the turbulence length scale behind uniform passive screens. However, the length scale value does not vary monotonically with either parameter but is observed to be affected by both.

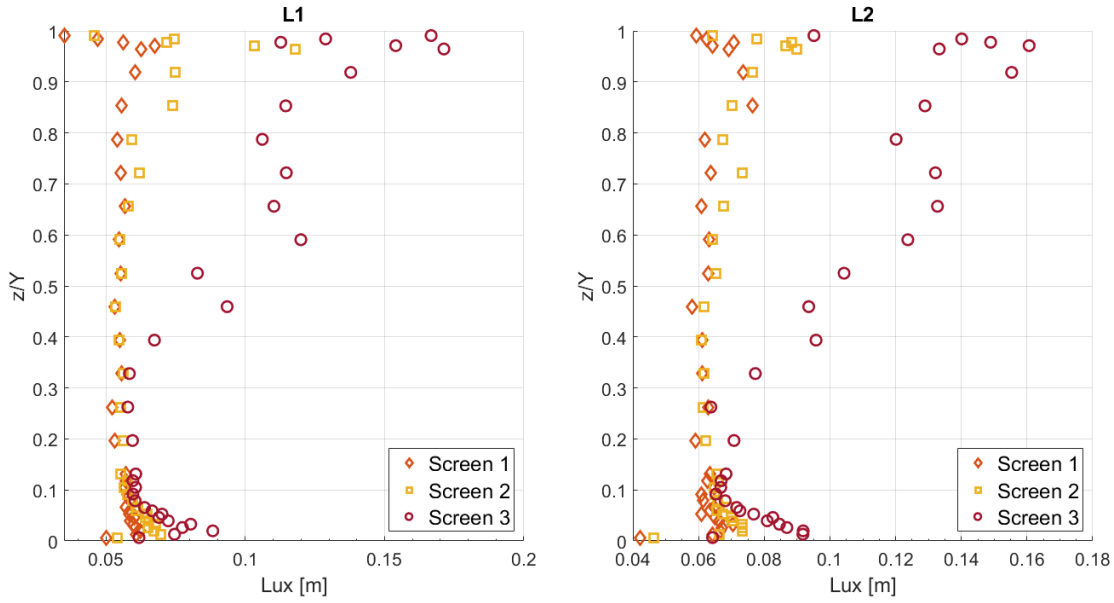

(a) L1, x/Y = 1.8 (b) L2, x/Y = 2.3

Figure 4. Turbulence length scale at L1 and L2 behind Grid 1, Screen 1, Screen 2, and Screen 3.

4. Conclusions

Experiments to generate shear flow fields using non-uniform porous screens were conducted in the open-circuit wind tunnel in the School of Civil Engineering at The University of Queensland. Three different shear flow fields were generated using rectangular grids with non-uniform porosities and a uniform flow field with a square grid was also tested. The mean velocity field and turbulence characteristics were investigated behind each of these screens. A deviation from the theoretical target mean shear velocity profiles were observed for each case, with the relative error increasing with the prescribed shear. Turbulence intensity and integral length scales were also measured behind each screen, with differences between screens only observed for the most highly sheared flow case. Future work will explore the development of a correction to the Choi et al. (2016) theoretical model to account for noted different levels of shear in the prescribed target mean velocity profile.

References

Butler, K., Kareem, A., Cao, S. & Tamura, Y. 2009, Analysis of the Surface Pressure Characteristics of Prismatic Models in Gust Front and Downburst Outflows, in *11th Americas Conference on Wind Engineering*, 22-29.

Choi, M. K., Lim, Y. B., Lee, H. W., Jung, H. & Lee, J. W. 2014, Flow uniformizing distribution panel design based on a non-uniform porosity distribution, *Journal of Wind Engineering and Industrial Aerodynamics*, **130**, 41-47.

Choi, M. K., Cho, M. K., Lee, H. W., Jung, H. & Lee, J. W. 2016, Generalized equation for the design of a baffle to generate arbitrary flow velocity profiles, *Journal of Wind Engineering and Industrial Aerodynamics*, **149**, 30-34.

Lin, W. E. & Savory, E. 2006, Large-scale quasi-steady modelling of a downburst outflow using a slot jet, *Wind and structures*, **9**, 419-440.

Mason, M., Li, Y. & Lo, Y. L. 2020, Wind Loads on the CAARC High-Rise Building Subject to Non-Traditional Boundary Layer Profiles, in *22nd Australasian Fluid Mechanics Conference AFMC2020, Brisbane, Australia*.

Vita, G., Hemida, H., Andrianne, T., & Baniotopoulos, C. C. 2018, Generating atmospheric turbulence using passive grids in an expansion test section of a wind tunnel, *Journal of Wind Engineering and Industrial Aerodynamics*, **178**, 91-104.

Zhang, Y & Mason, M. 2022, Wind Tunnel Investigation of Wall-bounded Flow behind Non-uniform Porous Screens, in 23rd Australasia*n Fluid Mechanics Conference AFMC2022, Sydney, Australia*.